HETEROCYCLES, Vol. 85, No. 8, 2012, pp. 1961 - 1973. © 2012 The Japan Institute of Heterocyclic Chemistry
Received, 22nd May, 2012, Accepted, 20th June, 2012, Published online, 27th June, 2012
DOI: 10.3987/COM-12-12514

ABSOLUTE CONFIGURATION OF THE MERODITERPENOIDS TAONDIOL AND EPITAONDIOL DIACETATES BY VIBRATIONAL CIRCULAR DICHROISM

Marcelo A. Muñoz,[a] Carlos Areche,[b] Juana Rovirosa,[b] Aurelio San Martín,[b] Bárbara Gordillo-Román,[c] and Pedro Joseph-Nathan*[,c]

[a]Instituto de Ciencias Químicas, Facultad de Ciencias, Universidad Austral de Chile, Casilla 567, Valdivia, Chile. [b]Departamento de Química, Facultad de Ciencias, Universidad de Chile, Casilla 653, Santiago, Chile. [c]Departamento de Química, Centro de Investigación y de Estudios Avanzados del Instituto Politécnico Nacional, Apartado 14-740, México, D. F., 07000 México. pjoseph@nathan.cinvestav.mx

Abstract – The absolute configuration of alga meroditerpenoids (–)-taondiol diacetate (**1b**) and (+)-epitaondiol diacetate (**2c**) are assigned by vibrational circular dichroism (VCD). The spectra of (2*S*,3*S*,6*R*,7*R*,10*R*,11*R*,14*S*)-**1b** and (2*S*,3*S*,6*S*,7*S*,10*R*,11*R*,14*S*)-**2c** enantiomers, calculated at the B3LYP/DGDZVP and at the B3LYP/DGDZVP2 levels of theory, respectively, matched confidently with the experimental ones. The numerical approach using neighborhood similarity indexes in the Compare*VOA* algorithm software supports the assignments with 100% confidence. The X-ray diffraction structures of **1b** and **2c** were determined to verify their relative stereochemistry and the crystal stereostructure of the meroditerpenoid stypotriol triacetate (**5**) is also reported.

INTRODUCTION

Isomeric polycyclic meroditerpenoids **1**-**4**, isolated from marine alga *Taonia atomaria* (Dictyotaceae),[1,2] brown alga *Stypopodium zonale* (Lamouroux) Pappenfuss (family Dictyotaceae),[3,4] marine alga *Stypopodium flabelliforme* Weber van Bosse (family Dictyotaceae),[5] and brown alga *Stypopodium flabelliforme* (Phaeophyceae)[6] are molecules with seven chiral centers, thereby allowing 64 possible pairs

of enantiomers. This structural complexity along with their mixed biogenesis, have made meroditerpenoids good markers for alga chemotaxonomic classification.[1,2,7-9]

Taondiol (**1a**) was the first meroditerpenoid isolated,[1,2,10,11] and the most frequently used in chemical transformations.[12-15] Its ichthyotoxicity and that of its derivatives are known.[3,16] Epitaondiol (**2a**) has shown anti-inflammatory and insecticidal activity[5,16] as well as strong antiviral activity against *Herpes simplex* virus HSV-1,[17] and 2β,3α-epitaondiol (**3**) displays moderate lung cancer cell line cytotoxicity.[6]

The originally published[3-5,7,9] 2β,3β,6α,7β relative stereochemistry of epitaondiol was reassigned to 2α,3β,6β,7α-**2a**, in light of 2D-NMR and NOEs of its methyl ether derivative (**2b**).[16] Based on this reassignment, the relative stereochemistry of epitaondiol diacetate (**2c**) has been corrected to 2α,3β,6β,7α.[18,19] However in CAS databases the incorrect 2β,3β,6α,7β stereochemistry is still retrieved upon calling its registry number [144539-75-3] with SciFinder®. Similarly, the originally published[5,6] 2β,3α,6α,7β relative stereochemistry of isoepitaondiol was reassigned to 2α,3α,6α,7β-**4a** considering 2D-NMR and single crystal X-ray diffraction of diacetate **4b**,[20] isolated from an acetylated dichloromethane extract of *S. flabelliforme*. Moreover, the absolute configuration (AC) of **4b** was assured to be 2*S*,3*R*,6*R*,7*R*,10*R*,11*R*,14*S* by vibrational circular dichroism (VCD),[20] a reliable spectroscopic technique in increasing use for AC determination of natural products in solution,[21-23] which was also used for the AC assignment of (3*S*,5*R*,8*R*,9*R*,10*S*,13*S*,14*S*)-stypotriol triacetate (**5**) a structurally related meroditerpenoid isolated from the Caribbean marine brown alga *S. zonale*.[24]

In this work, the AC of (−)-taondiol diacetate (**1b**) isolated from *S. flabelliforme*, collected from Easter Island, is assured to be (2*S*,3*S*,6*R*,7*R*,10*R*,11*R*,14*S*) using VCD spectroscopy. The optical rotation of **1b** matches with the previously reported value obtained after diacetylation of (−)-taondiol (**1a**) from *T. atomaria*,[2] whose stereochemistry was deduced by chemical correlation using commercial manool.[12] Contrarily, it mismatches with the partially racemized enantiomeric (+)-taondiol isolated from *S. zonale*,[3] also drawn with AC **1a**. Analogously, VCD is applied to investigate the AC of epitaondiol diacetate (**2c**). The X-ray crystal diffraction analyses of **1b** and **2c** are provided in support of their structures, along with the crystal structure of **5** to complete its stereochemical description.[24]

RESULTS AND DISCUSSION

The absolute configurations (ACs) of taondiol diacetate (**1b**) and epitaondiol diacetate (**2c**) were assessed by vibrational circular dichroism (VCD) in the infrared (IR) fingerprint region (950-1550 cm^{-1}). VCD of natural products acetate derivatives is common and has some advantages over the study of free alcohols which often show intermolecular solute-solute associations that complicate comparison of experimental and density functional theory (DFT) calculated spectra.[24,25]

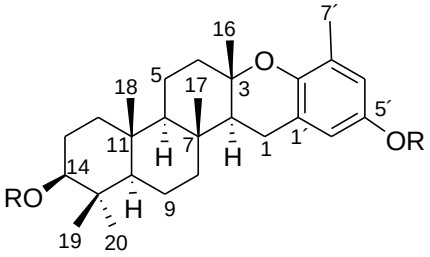

1a, R = H

1b, R = Ac

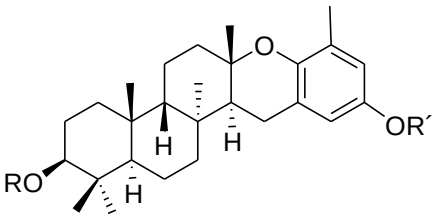

2a, R = R´ = H

2b, R = H, R´ = Me

2c, R = R´ = Ac

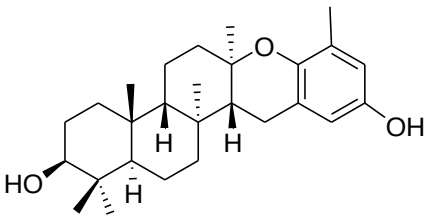

3

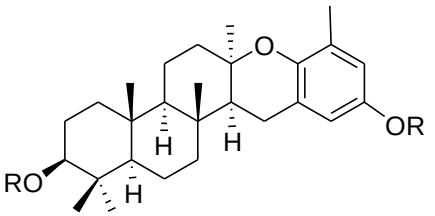

4a, R = H

4b, R = Ac

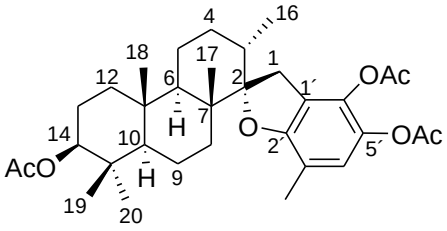

5

Diastereomeric meroditerpenoids taondiol diacetate (**1b**) and epitaondiol diacetate (**2c**) have 36 heavy atoms ($C_{31}H_{44}O_5$), 274 electrons and 234 active vibrations in the IR (Figures 1 and 2, respectively) and VCD spectra (Figures 3 and 4, respectively). VCD bands are monosignate signals or bisignate couplets, as those appearing at around 1150 cm^{-1} and 1200 cm^{-1}, belonging to the stretching ν_{CO} and bending δ_{CO} vibrations, respectively. The top line of Figures 1-4 corresponds to the observed spectra, while the bottom line corresponds to the DFT calculated spectra for (2*S*,3*S*,6*R*,7*R*,10*R*,11*R*,14*S*)-**1b** and (2*S*,3*S*,6*S*,7*S*,10*R*,11*R*,14*S*)-**2c** enantiomers at the B3LYP/DGDZVP and B3LYP/DGDZVP2 levels of theory, respectively.

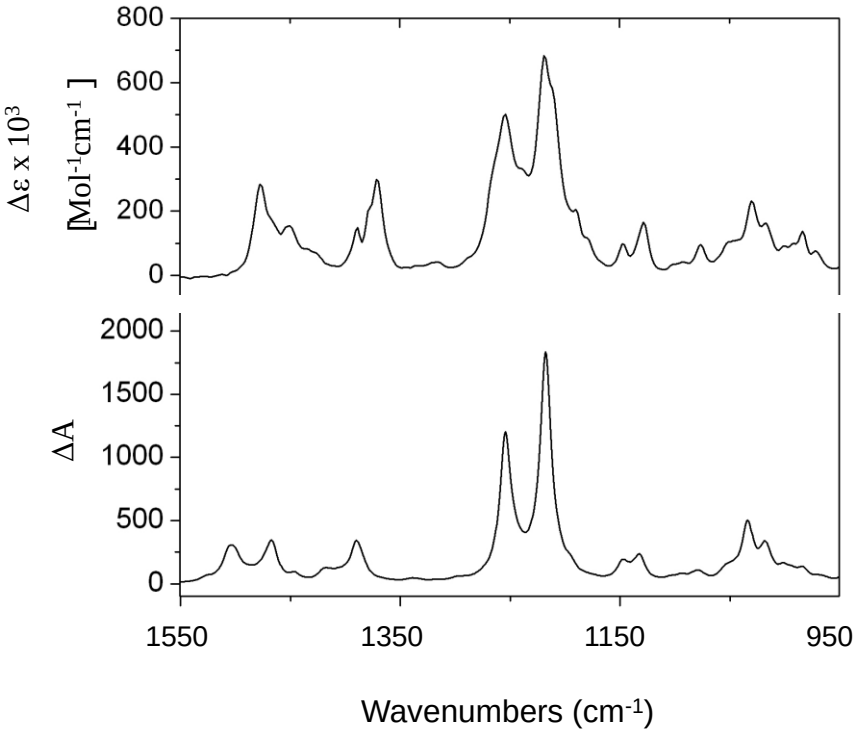

Figure 1. Comparison of the observed (top) and calculated (bottom) IR spectra of (2*S*,3*S*,6*R*,7*R*,10*R*,11*R*,14*S*)-**1b** obtained at the B3LYP/DGDZVP level of theory.

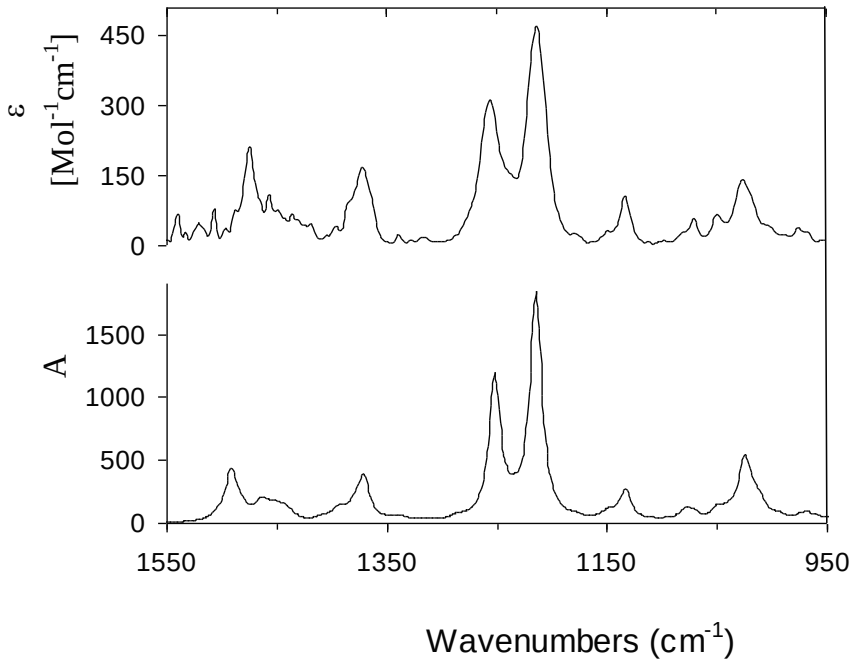

Figure 2. Comparison of the observed (top) and calculated (bottom) IR spectra of (2*S*,3*S*,6*S*,7*S*,10*R*,11*R*,14*S*)-**2c** obtained at the B3LYP/DGDZVP2 level of theory.

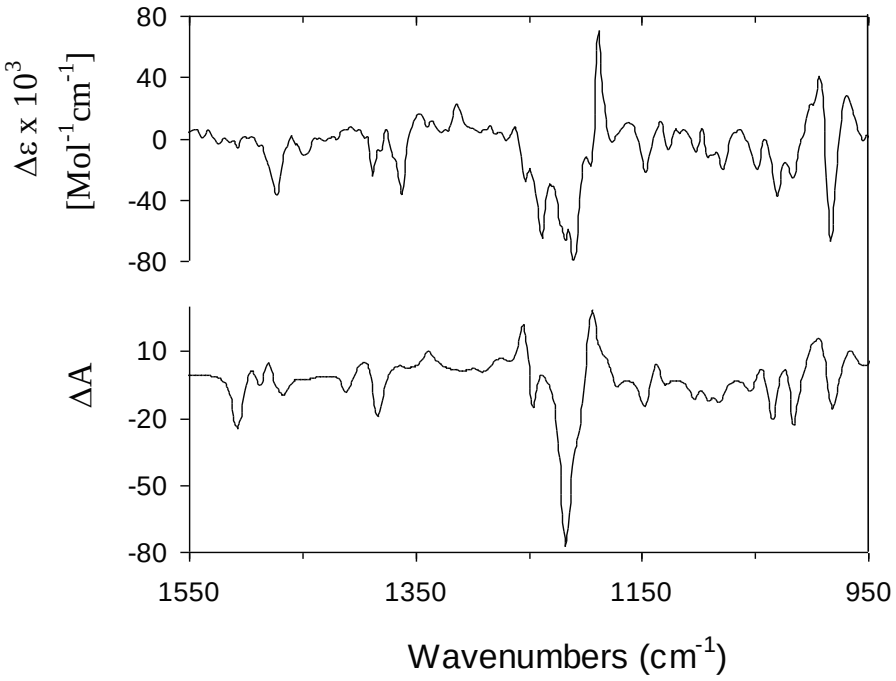

Figure 3. Comparison of the observed (top) and calculated (bottom) VCD spectra of (2*S*,3*S*,6*R*,7*R*,10*R*,11*R*,14*S*)-**1b** obtained at the B3LYP/DGDZVP level of theory.

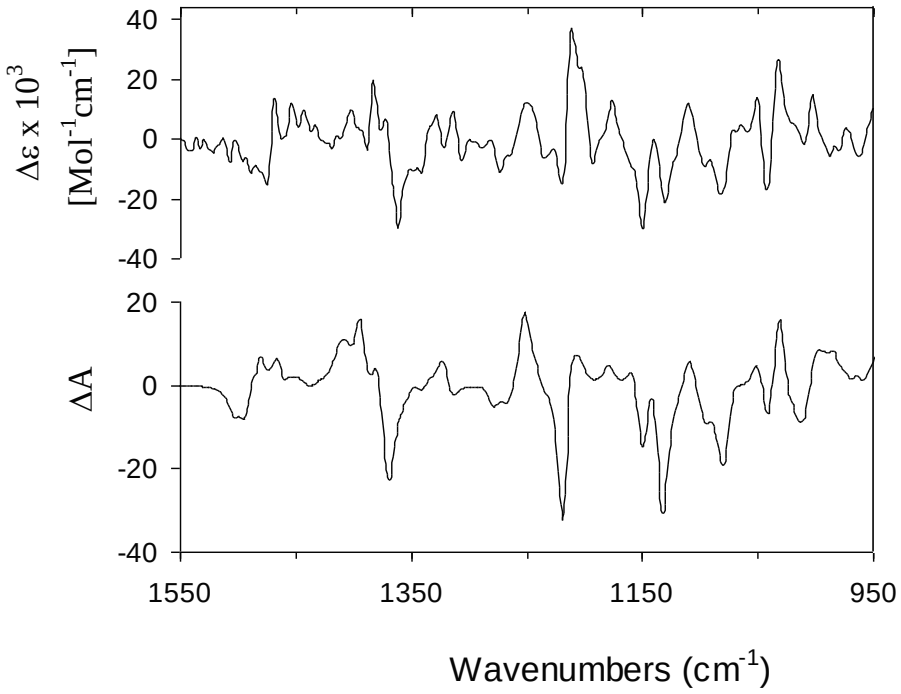

Figure 4. Comparison of the observed (top) and calculated (bottom) VCD spectra of 2*S*,3*S*,6*S*,7*S*,10*R*,11*R*,14*S*)-**2c** obtained at the B3LYP/DGDZVP2 level of theory.

In the IR and VCD spectra calculations, a weighted average of low-lying conformers was taken into consideration for each case. The search for the conformational distribution was started using the Monte Carlo MMFF94 molecular mechanics method, setting a 10 kcal/mol window in the Spartan'04 (Wavefunction, Irvine CA, USA) software. Twelve conformers were found for **1b** and seventeen for **2c**, however only two conformers account for 99.9% of the total population in the first 0.13 kcal/mol for **1b**, the third conformer being 4.6 kcal/mol above the first conformer. Similarly, for **2c** the 99.8% set of conformers were two in the first 0.14 kcal/mol, the third conformer being 4.3 kcal/mol above the first conformer. The energy data and Boltzmann population are summarized in Table 1. Single point calculations carried at the DFT B3LYP/DGDZVP level of theory for all **1b** and **2c** conformers assisted both assignment of the global minimum conformer and confirmation of conformer collection. Thus for **1b** the second conformer was separated by 0.2 kcal/mol from the global minimum and the third conformer by 4.2 kcal/mol, meanwhile for **2c**, the second conformer was separated by 0.1 kcal/mol and the third by 3.6 kcal/mol. The optimization of the two lowest-energy conformers for **1b** and **2c** was performed by DFT at the B3LYP/DGDZVP and B3LYP/DGDZVP2 levels of theory, respectively, using the Gaussian 03W program (Gaussian Inc., Pittsburg, PA, USA).

Table 1. Monte Carlo calculated relative energies and populations (%), single point (SP) relative energies and populations (%) at the B3LYP/DGDZVP level, and relative free energies (ΔG°) and populations (%) at the B3LYP/DGDZVP level for taondiol diacetate (**1b**) and at the B3LYP/DGDZVP2 level for epitaondiol diacetate (**2c**) conformers.

Diastereomer-*conformer*	[a]ΔE_{MMFF94} (kcal/mol)	% $_{MMFF94}$	[a]ΔE_{SP} (kcal/mol)	% $_{SP}$	[a] $\Delta\Delta G_{OPT}$ (kcal/mol)	[b] % $_{OPT}$
1b-*a*	[c] 0.00	55.4	[d] 0.00	58.4	[e] 0.00	81.1
1b-*b*	0.13	44.6	0.20	41.6	0.86	18.9
2c-*a*	[f] 0.00	55.7	[g] 0.00	53.2	[h] 0.00	55.0
2c-*b*	0.14	44.3	0.08	46.8	0.12	45.0

[a] Relative to the lowest energy conformer. [b] Calculated using the optimized free energies of the relevant conformers. [c] E_{MMFF} = 121.88 kcal/mol. [d] DFT ΔE_{SP} = -994054.98 kcal/mol. [e] DFT ΔG_{OPT} = -993660.02 kcal/mol. [f] E_{MMFF} = 141.23 kcal/mol. [g] DFT ΔE_{SP} = -994040.17 kcal/mol. [h] DFT ΔG_{OPT} = -993783.53 kcal/mol.

The **1b** and **2c** skeletons differ in the C6 and C7 configuration at the B/C *trans* ring junction. Consequently, the preferred conformations of rings B and C are quite different in the two diastereomers. In taondiol diacetate 6α,7β–**1b**, rings B and C adopt chair conformations (Figure 5 left), while in epitaondiol diacetate 6β,7α–**2c**, rings B and C are in twist-boat conformations (Figure 5 right). The

arrangement of the acetyl groups at C14 and C5′ in conformers *a* and *b* of **1b** gave rise to two alternate structures which are close in geometry at C14 but are symmetry related through the aromatic ring plane at C5′. An equivalent situation is observed for conformers *a* and *b* of **2c**. Frequency analyses confirmed the global minimum conformer to be conformer *a* for **1b**, as well as conformer *a* for **2c**. The Gibbs free energy, at 298.15 K and 1 atm, and the conformer populations are listed in Table 1.

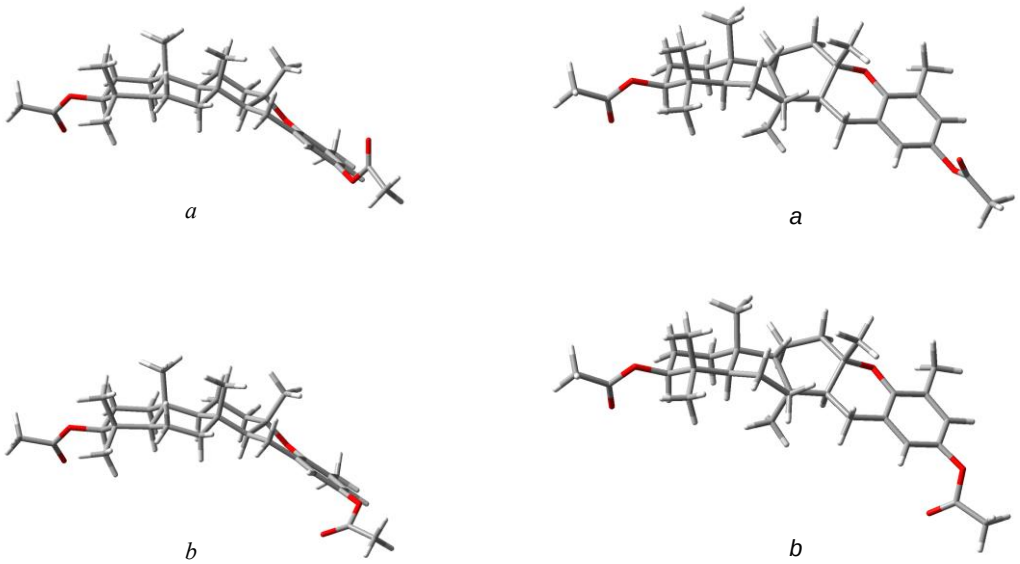

Figure 5. Geometry optimized conformers *a* and *b* of taondiol diacetate (**1b**) at the B3LYP/DGDZVP level of theory (left), and of epitaondiol diacetate (**2c**) at the B3LYP/DGDZVP2 level of theory (right).

The IR and VCD spectra intensities of **1b** and **2c** were determined by dipole strengths and rotational strengths using Lorentzian bandshapes with a bandwidth of $\nu = 6$ cm^{-1}. The weighted spectra, were calculated using the conformational abundances reported in Table 1. The matching of the weighted-to-observed spectra is visually exposed in Figures 1-4.

VCD bands are in fact a combination of several harmonic modes of coupled nuclei oscillations where CH vibrations of stereogenic centers make the higher contributions to the dissymmetric character observed in the VCD bands intensity.[26] Skeletal vibrations (1050-1150 cm^{-1} region) are more intense for **2c** (Figure 4) than for **1b** (Figure 3) disclosing the higher fused ring system dissymmetry of the former molecule. The configuration change at C6 and C7 is evident from the bands pattern of the stretching ν_{CH} and δ_{CH} deformations in the 1300-1500 cm^{-1} region. According to the visual VCD comparisons shown in Figures

3 and 4, there is a good concordance in sign and intensity between observed and calculated spectra allowing assignment of stereogenic centers for **1b** and **2c** to be trustful.

Furthermore, a higher confidence AC assignment was carried out by numerical neighborhood similarity (NS) analyses using the Compare*VOA* software package (BioTools, Jupiter, FL).[27] The NS provides the optimized frequency scaling as an anharmonicity factor (an*H*) for each comparison (Table 2). The calculated an*H* values are 0.985 for **1b** and 0.982 for **2c**. The reason to choose the DGDZVP2 basis set for **2c** is that a 100% confidence AC assignment was obtained, while a poorer AC confidence value (85%) was obtained using DGDZVP (Table 2). The optimized an*H* values for **1b** and **2c** were applied to the weighted IR and VCD spectra. Included in Table 2 are the previously unreported NS indexes for isoepitaondiol diacetate (**4b**)[20] and stypotriol triacetate (**5**),[24] which strengthen the AC assignments published after visual VCD spectra comparison.

Table 2. Confidence level data for the IR and VCD spectra of taondiol diacetate (**1b**), epitaondiol diacetate (**2c**), isoepitaondiol diacetate (**4b**),[18] and stypotriol triacetate (**5**).[22]

Cpd.	Method	[a] *anH*	[b] S_{IR}	[c] S_E	[d] S_{-E}	[e] *ESI*	[f] *C*
1b	B3LYP/DGDZVP	0.985	95.3	82.0	18.3	63.7	100
2c	B3LYP/DGDZVP	0.981	94.5	67.5	24.5	43.0	85
2c	B3LYP/DGDZVP2	0.982	97.0	71.1	21.2	50.0	100
4b	B3LYP/DGDZVP	0.983	95.1	77.4	23.7	53.6	100
5	B3LYP/DGDZVP	0.995	83.5	74.4	18.9	55.4	100

[a] Anharmonicity factor. [b] IR spectoscopic similarity. [c] VCD spectroscopic similarity for the correct enantiomer. [d] VCD spectroscopic similarity for the incorrect enantiomer. [e] Enantiomer similarity index, calculated as the S_E - S_{-E} difference. [f] Confidence level for the stereochemical assignment.

The agreement between the calculated and experimental IR spectra was assessed through the similarity index (S_{IR}), whose values 95.3, 97.0 and 95.1 for **1b**, **2c**, and **4b**, respectively, confirm the reliability of the theoretical methodology used to simulate the global spectra for each diastereomer. In the case of **5** the decreased S_{IR} value of 83.5 seems to be associated to the higher conformational freedom of triacetate **5** with six low-lying conformers[25] as compared to diacetates **1b**, **2c**, and **4b**[20] with only two populated conformers.

The VCD similarity indexes for the correct (S_E) and the incorrect (S_{-E}) enantiomers and the enantiomeric difference (*ESI*) measure the degree of success in the AC assignment. Thus for **1b**, the (2*S*,3*S*,6*R*,7*R*,10*R*,11*R*,14*S*) AC is supported by an S_E value of 82.0 allowing to discard the (2*R*,3*R*,6*S*,7*S*,10*S*,11*S*,14*R*) AC with an S_{-E} value of 18.3. With regard to (+)-epitaondiol diacetate (**2c**), neighborhood similarities S_E of 71.1 for (2*S*,3*S*,6*S*,7*S*,10*R*,11*R*,14*S*) and S_{-E} of 21.2 for its

(2*R*,3*R*,6*R*,7*R*,10*S*,11*S*,14*R*) antipode suggest the first to be the correct AC. This assignment is also assisted by an enatiomeric *ESI* difference of 50.0 and confirmed with a 100% confidence level reliability. In **4b** and **5** the experimental to calculated visual VCD spectra comparison provided the AC to be (2*S*,3*R*,6*R*,7*R*,10*R*,11*R*,14*S*),[20] and (3*S*,5*R*,8*R*,9*R*,10*S*,13*S*,14*S*),[24] respectively. Data summarized in Table 2 indicate that the numerical similarity indexes S_E and S_{-E} for **4b** which are 77.4 and 23.7, respectively, or 74.4 and 18.9, respectively, for **5**, validate the visual AC assessments.

The solid state structures of **1b**, **2c** and **5** obtained by single crystal X-ray diffraction are shown in Figure 6. Data were collected at room temperature for **2c** and **5**, however elusive collection data for a very weak monocrystal of **1b** forced the analysis to be done at low temperature. A summary of selected crystal data and structure determination parameters is presented in Table 3. The 2α,3β,6α,7β,10α,11β,14β, relative stereochemistry of **1b** is in agreement to the reported X-ray stereostructure of taondiol monoacetate,[28] and the stereochemistry of **2c** is 2α,3β,6β,7α,10α,11β,14β. The A/B/C ring system for **1b**, with two di-*eq-trans* junctions at C6α,C7β and C10α,C11β, displays a chair/chair/chair pattern, while the two di-*eq-trans* C6β,C7α and C10α,C11β junctions for **2c** force the A/B/C rings to be chair/twist-boat/twist-boat, as in calculated structures (Figure 5). The dihydrobenzopyran moiety is *quasi*-planar in the aromatic side but with alternate bonds involving the methylene C1 group in both diastereomers. The acetyl groups at C14 and at C5′ are in rotameric different arrangements than those in calculated conformers *a* or *b*. The X-ray diffraction stereostructure of stypotriol triacetate (**5**) shows the A/B/C rings geometry as in **1b**, even though the complete meroditerpenoid skeleton is different. The relative stereochemistry of **5** is 3β,5α,8β,9α,10β,13β,14β which validates its previously reported AC assignment by VCD as 3*S*,5*R*,8*R*,9*R*,10*S*,13*S*,14*S*.[24]

EXPERIMENTAL

General Experimental Procedures. The brown alga *Stypopodium flabelliforme* was collected intertidally near Hanga Roa, Rapa Nui, at Easter Island, Chile (South Pacific Ocean). Extraction and isolation of **1b** and **2c** have been reported elsewhere.[5,18,19,28] The optical rotations were determined on a Perkin Elmer 341 polarimeter at 20 ^{o}C. The IR and VCD measurements were performed on a BioTools Chiral*IR* FT-VCD spectrophotometer equipped with dual photoelastic modulation and a long-term detector. The compounds stability during VCD studies was verified by 300 MHz ^{1}H NMR prior and after VCD measurements. Single crystal X-ray diffraction data were collected on an Enraf-Nonius CAD4 diffractometer equipped with CuKα radiation (λ = 1.54184 Å) at 293(2) K in the ω-2θ scan mode or on a Bruker Smart 6000 CCD diffractometer equipped with MoKα radiation (λ = 0.7073 Å) and a low-temperature accessory.

Optical rotations. For taondiol diacetate (**1b**): $[\alpha]_D$ -37.4, $[\alpha]_{578}$ -41.8, $[\alpha]_{546}$ -47.7, $[\alpha]_{436}$ -83.4, *c* 0.65 $CHCl_3$. Lit.[2] $[\alpha]_D$ -56, *c* 0.82 $CHCl_3$. For epitaondiol diacetate (**2c**): $[\alpha]_D$ +44, $[\alpha]_{578}$ +47, $[\alpha]_{546}$ +52, $[\alpha]_{436}$ +80, *c* 0.44 $CHCl_3$.

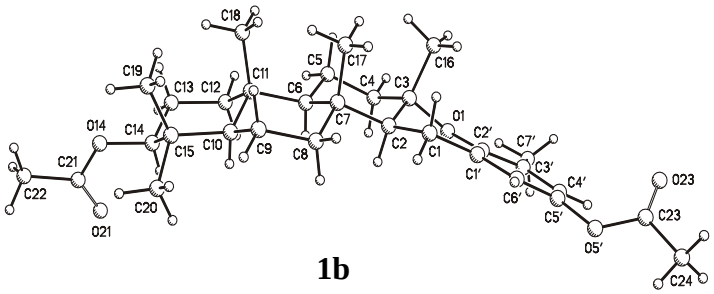

1b

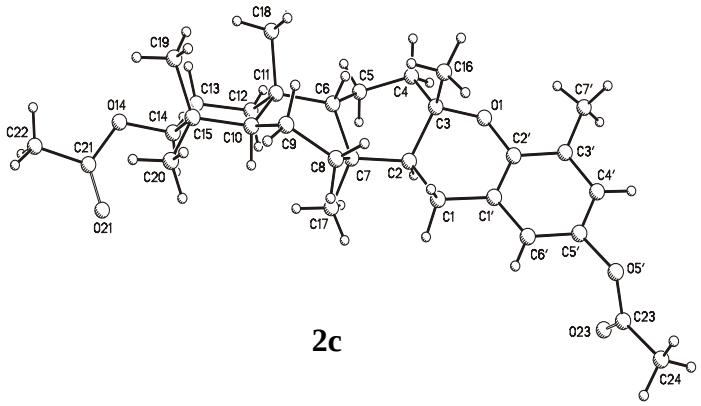

2c

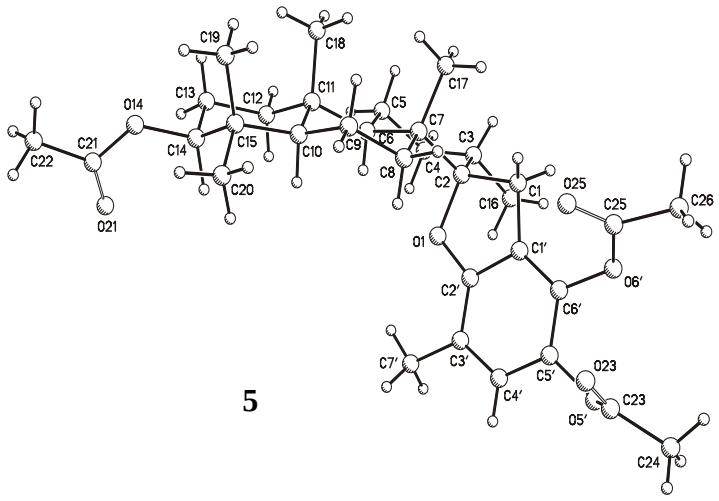

5

Figure 6. Single crystal X-ray structures of taondiol diacetate (**1b**), isoepitaondiol diactetate (**2c**) and stypotriol triacetate (**5**).

Table 3. Crystal data, structure solution and refinement parameters for (−)-taondiol diacetate (**1b**), (+)-epitaondiol diacetate (**2c**) and stypotriol triacetate (**5**).

Compound	**1b**	**2c**	**5**
Formula	$C_{31}H_{44}O_5$	$C_{31}H_{44}O_5$	$C_{33}H_{46}O_7$
Molecular weight	496.66	496.66	554.70
T (K)	173(2)	293(2)	293(2)
Size (mm)	0.18x0.10x0.05	0.38x0.32x0.32	0.24x0.06x0.04
Wavelength (Å)	0.71073	1.54184	1.54184
Crystal system	monoclinic	orthorhombic	orthorhombic
Space group	$P2_1$	$P2_12_12_1$	$P2_12_12_1$
a (Å)	7.337(2)	11.227(4)	11.463(1)
b (Å)	11.129(2)	14.034(2)	12.546(3)
c (Å)	17.510(4)	17.668(2)	21.631(1)
β (°)	98.92(3)	90	90
V (Å^3)	1412.5(6)	2783.7(12)	3110.8(9)
D_{calcd} (g cm^{-3})	1.168	1.185	1.184
Z	2	4	4
M (mm^{-1})	0.077	0.623	0.659
F000	540	1080	1200
θ_{range} (°)	2.98 – 26.91	5.01 - 59.93	4.09 – 59.94
Refl total	10878	2094	2432
Refl. Unique	5435	2013	2317
R_{int} (%)	0.1772	0.0001	0.0001
Refl. observ.	2212	1965	1395
Param. Refined	334	342	378
R (%), R_w (%)	8.2, 14.0	3.8, 10.8	6.9, 17.4
e_{max} (eÅ^{-3})	0.216	0.168	0.196

VCD measurements. Samples of 9.7 mg of (−)-taondiol diacetate (**1b**) and 7.8 mg of (+)-epitaondiol diacetate (**2c**) were dissolved in 150 μL of 100% atom-D $CDCl_3$. The solutions were placed in a BaF_2 cell having a pathlength of 100 μm and data were acquired at a resolution of 4 cm^{-1} during 4 and 14 h, respectively. Base line corrections were done by subtracting the solvent spectrum acquired under identical instrument conditions.

Molecular Modeling and VCD Calculations. Geometry optimizations for both **1b** and **2c** were performed using MMFF94 force-field calculations as implemented in the Spartan'04 program using the X-ray atom coordinates as starting values. A Monte Carlo search protocol was carried out considering an energy cut-off of 10 kcal/mol providing 12 and 17 conformers for **1b** and **2c**, respectively, with only two highly populated conformers for each diastereoisomer. Single point calculations using the DFT B3LYP/DGDZVP level of theory for all conformers confirmed conformer population. The two lowest-energy conformers were optimized at the B3LYP/DGDZVP level of theory for **1b**, and at the B3LYP/DGDZVP2 level for **2c** using Gaussian 03W software. The relative MMFF and DFT energies, and populations of these two conformers are compiled in Table 1. The minimized structures were used to calculate the thermochemical parameters and the IR and VCD frequencies at 298 K and 1 atm. Molecular visualization was carried out in the GaussianView 3.0 program. Calculations for **1b** required between 163 and 197 h of CPU time per conformer and those for **2c** required between 215 and 280 h when using a desktop personal computer with 2 Gb RAM operated at 3 GHz.

X-Ray diffraction analyses. The collected reflections were corrected for background, Lorentz polarization, and absorption, while crystal decay was negligible. The structures were solved by direct methods using the SHELXS-97 program. For the structural refinement, the non-hydrogen atoms were treated anisotropically, and the hydrogen atoms were refined isotropically. The final R indexes and other relevant crystal data **1b**, **2c** and **5** are summarized in Table 3. Crystallographic data are deposited with the Cambridge Crystallographic Data Centre. Deposition numbers are CCDC-885984 for **1b**, CCDC-885985 **2c**, and CCDC-885986 for **5**. Free copies of the data can be obtained via http://www.ccdc.cam.ac.uk/conts/retrieving.html (or from the Cambridge Crystallographic Data Centre, 12 Union Road, Cambridge, CB2 1EZ, UK; Fax: +44 1223 336033; e-mail: deposit@ccdc.cam.ac.uk).

ACKNOWLEDGEMENTS

Partial financial support from CONACyT-México grant 152994 is greatly appreciated.

REFERENCES

1. A. G. González, J. Darías, and J. D. Martín, *Tetrahedron Lett.*, 1971, **12**, 2729.
2. A. G. González, J. Darías, J. D. Martín, and C. Pascual, *Tetrahedron*, 1973, **29**, 1605.
3. W. H. Gerwick and W. Fenical, *J. Org. Chem.*, 1981, **46**, 22.
4. W. H. Gerwick, W. Fenical, and J. N. Norris, *Phytochem.*, 1985, **24**, 1279.
5. J. Rovirosa, M. Sepulveda, E. Quezada, and A. San-Martín, *Phytochem.*, 1992, **31**, 2679.
6. O. M. M. Sabry, S. Andrews, K. L. McPhail, D. E. Goeger, A. Yokochi, K. T. LePage, T. F. Murray, and W. H. Gerwick, *J. Nat. Prod.*, 2005, **68**, 1022.

7. A. G. González, M. A. Alvarez, J. D. Martín, M. Norte, C. Pérez, and J. Rovirosa, *Tetrahedron*, 1982, **38**, 719.
8. A. R. Soares, V. L. Teixeira, R. C. Pereira, and R. Villaça, *Biochem. System. Ecol.*, 2003, **31**, 1347.
9. A. R. Soares, B. A. P. da Gama, A. P. da Cunha, V. L. Teixeira, and R. C. Pereira, *Marine Biotech.*, 2008, **10**, 158.
10. A. G. González, J. Darias, and J. D. Martín, *An. Quim.*, 1972, **68**, 1187.
11. A. G. González, J. D. Martín, C. Pérez, and J. Rovirosa, *Bol. Soc. Chil. Chem.*, 1982, **27**, 168.
12. A. G. González and J. D. Martin, *Tetrahedron Lett.*, 1972, **13**, 2259.
13. A. G. González, M. A. Alvarez, J. Darias, and J. D. Martín, *J. Chem. Soc., Perkin Trans. 1*, 1973, 2637.
14. A. S. Kumanireng, T. Kato, and Y. Kitahara, *Chem. Lett.*, 1973, **10**, 1045.
15. P. F. Vlad and N. D. Ungur, *Chem. Nat. Prod.*, 1986, **22**, 369.
16. F. Sánchez-Ferrando and A. San-Martín, *J. Org. Chem.*, 1995, **60**, 1475.
17. A. R. Soares, J. L. Abrantes, T. M. L. Souza, C. F. L. Fontes, R. C. Pereira, and I. C. de P. P. Frugulhetti, *Planta Med.*, 2007, **73**, 1221.
18. D. M. Pereira, J. Cheel, C. Areche, A. San-Martín, J. Rovirosa, L. R. Silva, P. Valentao, and P. B. Andrade, *Mar. Drugs*, 2011, **9**, 852 (see *Chem. Abstr.*, 2011, **155**, 504926).
19. C. Areche, A. San-Martín, J. Rovirosa, J. Soto-Delgado, and R. Contreras, *Phytochem.*, 2009, **70**, 1315 (see *Chem. Abstr.*, 2009, **151**, 398492).
20. C. Areche, A. San-Martín, J. Rovirosa, M. A. Muñoz, A. Hernández-Barragán, M. A. Bucio, and P. Joseph-Nathan, *J. Nat. Prod.*, 2010, **73**, 79.
21. L. A. Nafie, *Nat. Prod. Commun.*, 2008, **3**, 451.
22. P. L. Polavarapu, 'Determination of the Structures of Chiral Natural Products Using Vibrational Circular Dichroism', in 'Comprehensive Chiroptical Spectroscopy: Stereochemical Analysis of Synthetic Compounds, Natural Products, and Biomolecules', Vol. 2, ed. by N. Berova, P. L. Polavarapu, K. Nakanishi, and R. W. Woody, Wiley, New York, 2012, pp. 387-420.
23. H. Yanan, B. Wang, and R. K. Dukor, *Appl. Spect.*, 2011, **65**, 699.
24. M. A. Muñoz, C. Areche, A. San-Martín, J. Rovirosa, and P. Joseph-Nathan, *Nat. Prod. Commun.*, 2009, **4**, 1037.
25. N. H. Andersen, N. J. Christensen, P. R. Lassen, T. B. N. Freedman, L. A. Nafie, K. Strømgaard, and L. Hemmingsen, *Chirality*, 2010, **22**, 217.
26. B. Gordillo-Román, J. Camacho-Ruiz, M. A. Bucio, and P. Joseph-Nathan, *Chirality*, 2012, **24**, 147.
27. E. Debie, E. De Gussem, R. K. Dukor, W. Herrebout, L. A. Nafie, and P. Bultinck, *Chem. Phys. Chem. Special Issue: Jacobus van't Hoff*, 2011, **12**, 1542.
28. K. Peters, E.-M. Peters, and H. G. von Schnering, *Zeits. Kristall.*, 1996, **211**, 71.